Distinct Neuronal Projections From the Hypothalamic Ventromedial Nucleus Mediate Glycemic and Behavioral Effects

Chelsea L. Faber,[1] Miles E. Matsen,[1] Kevin R. Velasco,[1] Vincent Damian,[1] Bao Anh Phan,[1] Daniel Adam,[2] Anthony Therattil,[3] Michael W. Schwartz,[1] and Gregory J. Morton[1]

Diabetes 2018;67:2518–2529 | https://doi.org/10.2337/db18-0380

The hypothalamic ventromedial nucleus (VMN) is implicated both in autonomic control of blood glucose and in behaviors including fear and aggression, but whether these divergent effects involve the same or distinct neuronal subsets and their projections is unknown. To address this question, we used an optogenetic approach to selectively activate the subset of VMN neurons that express neuronal nitric oxide synthase 1 (VMN^{NOS1} neurons) implicated in glucose counterregulation. We found that photoactivation of these neurons elicits *1*) robust hyperglycemia achieved by activation of counterregulatory responses usually reserved for the physiological response to hypoglycemia and *2*) defensive immobility behavior. Moreover, we show that the glucagon, but not corticosterone, response to insulin-induced hypoglycemia is blunted by photoinhibition of the same neurons. To investigate the neurocircuitry by which VMN^{NOS1} neurons mediate these effects, and to determine whether these diverse effects are dissociable from one another, we activated downstream VMN^{NOS1} projections in either the anterior bed nucleus of the stria terminalis (aBNST) or the periaqueductal gray (PAG). Whereas glycemic responses are fully recapitulated by activation of VMN^{NOS1} projections to the aBNST, freezing immobility occurred only upon activation of VMN^{NOS1} terminals in the PAG. These findings support previous evidence of a VMN→aBNST neurocircuit involved in glucose counterregulation and demonstrate that activation of VMN^{NOS1} neuronal projections supplying the PAG robustly elicits defensive behaviors.

Although glucose is sensed in peripheral tissues, including pancreatic β-cells and the hepatic portal vein, the brain has the capacity to sense glucose both directly and indirectly (1–3). The brain also plays a key role in driving the counterregulatory responses (CRRs) to hypoglycemia, which include inhibition of insulin secretion and enhanced secretion of glucagon, corticosterone, and epinephrine (4). Hypoglycemia is both the most frequent complication of diabetes treatment and the major obstacle to achieving tight glycemic control in people with diabetes (5). Furthermore, a single severe bout of hypoglycemia increases the risk not only of cardiovascular disease and mortality but also of subsequent hypoglycemic episodes (6). Improving our understanding of the mechanisms by which hypoglycemia is sensed and responded to by the brain is therefore critical to the development of new, more effective strategies for diabetes treatment.

Although glucose counterregulation involves multiple brain areas (1), neurons in the hypothalamic ventromedial nucleus (VMN) appear to play an important role. This assertion is based on evidence that *1*) the VMN is activated during hypoglycemia (7), *2*) electrical stimulation of the VMN activates CRRs and raises blood glucose levels (8,9), and *3*) glucose delivery specifically within the VMN blunts CRRs during systemic hypoglycemia (10). Moreover, using an optogenetics approach, we recently demonstrated that activation of the subset of VMN neurons that express steroidogenic factor 1 (VMN^{SF1} neurons) activates CRRs and thereby raises blood glucose levels, whereas their inhibition blocks recovery from hypoglycemia (11). These data are in line with previous studies showing an impaired CRR to insulin-induced hypoglycemia when glutamate is deleted from VMN^{SF1} neurons (12), and with evidence that

[1]UW Medicine Diabetes Institute, Department of Medicine, University of Washington, Seattle, WA
[2]School of Medicine, Creighton University, Omaha, NE
[3]School of Medicine, New York Medical College, Valhalla, NY
Corresponding author: Gregory J. Morton, gjmorton@u.washington.edu.

Received 30 March 2018 and accepted 17 September 2018.

This article contains Supplementary Data online at http://diabetes.diabetesjournals.org/lookup/suppl/doi:10.2337/db18-0380/-/DC1.

projections from the lateral parabrachial nucleus to the VMN are essential to effective glucose counterregulation (13).

In addition to its role in glucose homeostasis, the VMN is implicated in the "fight or flight" response and associated behaviors, including fear/anxiety and aggression (14–16). In accordance with this concept, activation of VMN^{SF1} neurons elicits defensive behaviors, including freezing immobility and/or activity bursts, characteristic of a fearful emotional state (16,17). Since psychological stress could potentially contribute to hyperglycemia induced by VMN^{SF1} neuron activation, the current work was undertaken to determine if neurocircuitry downstream of the VMN involved in glucose counterregulation can be distinguished from that involved in defensive behaviors. Specifically, we hypothesized that these divergent responses involve discrete neuronal subsets within the VMN that project to distinct downstream brain regions. Consistent with this hypothesis, neurons located in the ventrolateral (vl) portion of the VMN are known to be involved in reproductive and aggressive behaviors (17,18), and neurons in the central (c) and dorsomedial (dm) VMN are implicated in both metabolic regulation (19,20) and defensive behaviors (16). Moreover, work from us and others has shown that VMN neurons project heavily to multiple brain areas, including the anterior bed nucleus of the stria terminalis (aBNST), an area implicated in autonomic control of homeostatic functions and stressor integration (21,22), and the periaqueductal gray (PAG), a brain region classically known for its role in fear and pain (23).

Based on work from Fioramonti et al. (24), we hypothesized a glucoregulatory role for neurons in the VMN expressing neuronal nitric oxide synthase 1 (VMN^{NOS1} neurons), a subset of VMN^{SF1} neurons. This hypothesis is supported by published evidence that *1*) VMN^{NOS1} neurons are responsive to a fall in glucose levels (7,25), *2*) hypoglycemia induces phosphorylation and activation of NOS1 (7,24), and *3*) pharmacological and genetic inhibition of NOS1 impairs epinephrine and glucagon responses to hypoglycemia and slows the recovery of blood glucose levels to normal (24). Based on these findings, we sought to determine *1*) if activation of VMN^{NOS1} neurons is sufficient and/or required for intact CRRs to hypoglycemia and *2*) if distinct projections from VMN^{NOS1} neurons mediate glycemic and behavioral responses or if instead the two responses are inextricably linked, as would be expected if the hyperglycemia is a manifestation of the behavioral response.

RESEARCH DESIGN AND METHODS

Animals

All procedures were performed in accordance with the National Institutes of Health *Guide for the Care and Use of Laboratory Animals* and were approved by the Animal Care Committee at the University of Washington. All studied animals were individually housed in a temperature-controlled room with a 12-h:12-h light:dark cycle under specific pathogen-free conditions and provided with ad libitum access to water and chow unless otherwise noted. Nos1-Cre mice and C57Bl/6J mice were purchased from The Jackson Laboratory (stock no. 017526 and 000664, respectively).

Viral Microinjection and Fiber Placement Surgeries

The viral vectors AAV5-EF1a-DIO-hChR2(H134R)-EYFP, AAVDJ8-EF1a-DIO-SwiChR$_{CA}$-TS-EYFP-WPRE, and AAV5-EF1a-DIO-EYFP used in this study have been previously described (11). All viruses were purchased from the Gene Therapy Center at the University of North Carolina except the SwiChR virus, which was provided by Karl Deisseroth (Stanford University, Stanford, CA) and packaged into a DJ8 vector by the University of Washington Diabetes Research Center Viral Vector and Transgenic Mouse Core. For viral microinjection, animals were placed in a stereotaxic frame (Kopf 1900; Cartesian Research Inc., Tujunga, CA) under isoflurane anesthesia. The skull was exposed with a small incision, and a small hole was drilled for unilateral 200-nL injection volume of AAV5-EF1a-DIO-hChR2(H134R)-EYFP, or 200-nL bilateral injection of the inhibitory AAVDJ8-EF1a-DIO-SwiChR$_{CA}$-TS-EYFP-WPRE, to the VMN of Nos1-Cre male mice based on slightly modified coordinates from the Mouse Brain Atlas: anterior-posterior (AP) −1.0 mm, dorsal-ventral (DV) −5.7 mm, and lateral 0.45 mm. Adeno-associated virus (AAV) was delivered using a Hamilton syringe with a 33-gauge needle at a rate of 50 nL/min (Micro4 controller), followed by a 7-min wait at the injection site and a 1-min wait 0.1 mm dorsal to the injection site before needle withdrawal. After viral injections, a fiber-optic ferrule (Doric Lenses, Quebec, Canada) was implanted above the VMN (AP −1.0 mm, DV −5.3 mm, lateral 0.45 mm), the aBNST (AP 0.86 mm, DV −4.4 mm, lateral 0.65 to the ipsilateral side), or the PAG (AP −4.2 mm, DV −2.2 mm, lateral 0.15 mm to the ipsilateral side) in separate cohorts of mice. For bilateral inhibition, fiberoptics were implanted at a 15° from center angle. Animals received a perioperative subcutaneous injection of buprenorphine hydrochloride (0.05 mg/kg) (Reckitt Benckiser, Richmond, VA). After surgery, mice were allowed 2 (for cell body stimulation) to 6 weeks (for terminal stimulation) to recover and to maximize viral expression. Mice were acclimated to handling and experimental conditions three times prior to the start of any in vivo studies. Viral expression and fiber placement were verified post hoc in all animals, and any data from animals in which the virus or fiber was located outside the targeted area were excluded from the analysis.

Optogenetic Photoactivation and Photoinhibition

Optogenetic studies were supported by the Nutrition Obesity Research Center (NORC) Energy Balance Core at the University of Washington. Light was delivered to the target area from a diode laser (473 nm, DPSS continuous wave laser system; Laserglow, Toronto, Ontario, Canada) controlled via pulse generator (Master-9; A.M.P.I., Jerusalem, IL) as previously described (11). In brief, the

output beam from the laser system was delivered through a single fiber port connected to a fiberoptic rotary joint (Doric Lenses). A terminal fiber attached to the rotary joint was connected to the indwelling fiberoptic cannula via a ceramic mating sleeve (Thor Laboratories, Newton, NJ). Unless otherwise noted, all photostimulation experiments used 5-ms pulses at 40 Hz with an estimated 3-mW light power exiting the fiber tip. Photoinhibition experiments used a constant beam of light for 1–2 h as indicated for each experiment. Irradiance at target regions is estimated at 7.82 mW/mm^2 based upon previously described light penetration through neural tissues (web.stanford.edu/group/dlab/cgi-bin/graph/chart.php).

Metabolic Studies and Tissue Processing

To investigate the effect of selective activation or inhibition of VMN^{NOS1} neurons on glycemic control, we used a 3-h approach with alternating laser off/on/off sequences in Nos1-Cre mice in a randomized, crossover manner, as previously described (11). Tail vein blood was collected for blood glucose levels at indicated times using a handheld glucometer (FreeStyle; Abbott, Santa Clara, CA). Tail blood for plasma hormonal measurement was collected at the end of the "Laser on" photoactivation (stimulation) or "Laser off" (mock) period (t = 60 min); for photoinhibition studies, blood samples for plasma hormonal measurement were collected at the end of the baseline period (t = 0) and during the study period (t = 60 min), as indicated. Tail blood was collected in EDTA-coated capillary tubes and centrifuged (10,000 rpm, 7 min), and plasma was subsequently removed and stored at −80°C for subsequent assay. Plasma insulin (Crystal Chem, Elk Grove Village, IL), corticosterone (ALPCO, Salem, NH), and glucagon (Mercodia, Winston-Salem, NC) were determined by ELISA.

Insulin-Induced Hypoglycemia

In two separate studies using insulin-induced hypoglycemia, 4 h–fasted animals received an intraperitoneal (i.p.) injection of human insulin (1.0 or 1.5 units/kg body weight; Humulin; Eli Lilly and Company, Indianapolis, IN) at t = 0 min. Tail vein blood was collected for measurement of blood glucose levels at −15, 0, 15, 30, 45, 60, 90, and 120 min using a handheld glucometer (Abbott) and blood samples collected for hormonal analysis as described above (11).

For studies evaluating c-Fos expression during insulin-induced hypoglycemia, C57Bl/6J mice were acclimated to handling and i.p. injections. On the study day, animals were fasted for 4 h prior to receiving an i.p. injection of insulin (1.5 units/kg body weight; Humulin; Eli Lilly and Company) or saline control. After 60 min, animals were anesthetized and perfused as described below. For quantification of c-Fos expression, Fiji was used to define a standard region of interest for three representative sections per animal spanning the aBNST (bregma 0.62–0.30 mm) and the PAG (bregma −4.16 to −4.36), respectively. In brief, images were converted to 16 bit and the threshold adjusted to minimize nonspecific background fluorescence. Cells were then identified and counted using the analyze particles feature, such that consistent fluorescence and size thresholds were used throughout, as previously described (26).

Immunohistochemistry

For brain immunohistochemical (IHC) studies, after 1 h of mock photoactivation or photoinhibition, animals were overdosed with ketamine:xylazine and perfused with PBS followed by 4% (volume for volume) paraformaldehyde in 0.1 mol/L PBS. Brains were removed and postfixed for 2–6 h, sucrose (30%) embedded, and subsequently frozen in optimal cutting temperature compound blocks. Free-floating coronal sections were obtained via Crysotat at 30 microns and stored in PBS with azide at 4°C for IHC staining.

c-Fos immunostaining was performed in free-floating sections. In brief, sections were put into PBS with Tween 20 (PBST) overnight at 4°C. Sections were then washed at room temperature in PBST (3 × 8 min), followed by a blocking buffer (5% normal goat serum, 1% BSA in 0.1 mol/L PBST with azide) for 60 min with rocking. Sections were then incubated overnight at 4°C with goat anti–c-Fos (sc-52-G, RRID:AB_2629503; Santa Cruz Biotechnology, Dallas, TX) diluted 1:500 in blocking buffer. Next, sections were washed (3 × 8 min) in PBST before incubating in secondary donkey anti-goat Alexa 594 (Jackson ImmunoResearch Laboratories, West Grove, PA) diluted 1:300. Sections were then mounted to slides and imaged using a Nikon Eclipse E600 upright microscope equipped with a Diagnostic Instruments Spot RT Color digital camera.

Behavioral Quantification

To avoid confounding stress responses, behavioral sessions were performed in the animals' home cages. All sessions were video recorded and subsequently analyzed with Ethovision (Noldus, Leesburg, VA) tracking software as previously described (27).

Statistical Analyses

All results are presented as means ± SEM. P values for pairwise comparisons were calculated by two-tailed Student t test. Time course comparisons between groups were analyzed using a two-way repeated-measures ANOVA with main effects of treatment (mock vs. stimulation or inhibition) and time. All post hoc comparisons were determined using Sidak correction for multiple comparisons. All statistical tests indicated were performed using Prism (version 7.4; GraphPad, La Jolla, CA) software.

RESULTS

Activation of VMN^{NOS1} Neurons Induces Hyperglycemia

To test the hypothesis that photoactivation of VMN^{NOS1} neurons is sufficient to engage CRRs and thereby raise blood glucose levels, Nos1-Cre^{+} mice received a unilateral

microinjection to the VMN of an AAV encoding either a YFP control or a Cre-dependent sodium-conducting channelrhodopsin fused with a fluorescent reporter [AAV5-EF1a-DIO-hChR2(H134R)-EYFP, hereafter called ChR2-YFP], followed by implantation of an optic fiber above the injection site (Fig. 1*A* and *B*). As expected, ChR2-YFP expression was largely restricted to the VMN and not adjacent nuclei (Fig. 1*C*). Activation of VMN neurons after photostimulation was further confirmed by increased expression of the immediate-early gene, c-Fos (Fig. 1*C*). As predicted, photoactivation of VMN^{NOS1} neurons rapidly elevated blood glucose levels, with levels returning to baseline within 1 h of termination of the light stimulus (Fig. 2*A*), an effect that recapitulates the response to photoactivation of VMN^{SF1} neurons (of which VMN^{NOS1} neurons are a subset) (11). Because this effect was not observed in Nos1-Cre^{+} animals that underwent the same light stimulation procedure, but had received a YFP control virus (Fig. 2*B*), we conclude that the observed glycemic responses were not due to nonspecific effects of blue light delivery to the VMN and instead reflect a specific response to activation of VMN^{NOS1} neurons. Moreover, our findings that there was little if any effect on blood glucose levels after photoactivation of Nos1 neurons in which viral and/or fiberoptic targeting was detected predominantly outside the VMN (data not shown) further strengthen our hypothesis that NOS1 neurons in the VMN, but not those in adjacent brain areas, have potent glucoregulatory effects.

Autonomic and Neuroendocrine Effects of VMN^{NOS1} Photoactivation

Based on the response to photoactivation of VMN^{SF1} neurons (11), we hypothesized a role for autonomic and neuroendocrine mechanisms engaged during glucose counterregulation in the hyperglycemic response to activation of VMN^{NOS1} neurons. Consistent with this hypothesis, we found that the effect of photoactivation of VMN^{NOS1} neurons to induce hyperglycemia (Fig. 2*A*, 60 min, shown in Fig. 2*C* as line graph) was associated with a marked rise in plasma levels of the counterregulatory hormones corticosterone and glucagon (Fig. 2*E* and *F*). The increase of glucagon levels is particularly notable in that although it plays a key role in glucose counterregulation, it is not typically a component of the nonspecific response to fear-inducing stimuli (28). Further, plasma insulin levels failed to increase, despite marked hyperglycemia, indicating potent autonomic suppression of glucose-stimulated insulin secretion (GSIS) (Fig. 2*D*). These cardinal features of the CRR fully recapitulate the effects of VMN^{SF1} activation.

Behavioral Effects of VMN^{NOS1} Photoactivation

Consistent with the known role of the VMN in mediating defensive behaviors, we found that in addition to glycemic effects (Fig. 2*A*–*F*), freezing immobility behavior was observed throughout the entire period during which VMN^{NOS1} neurons were activated (Fig. 2*G* and Supplementary Video 1). This effect was quantified as an increase in overall time spent immobile (Fig. 2*H*) and

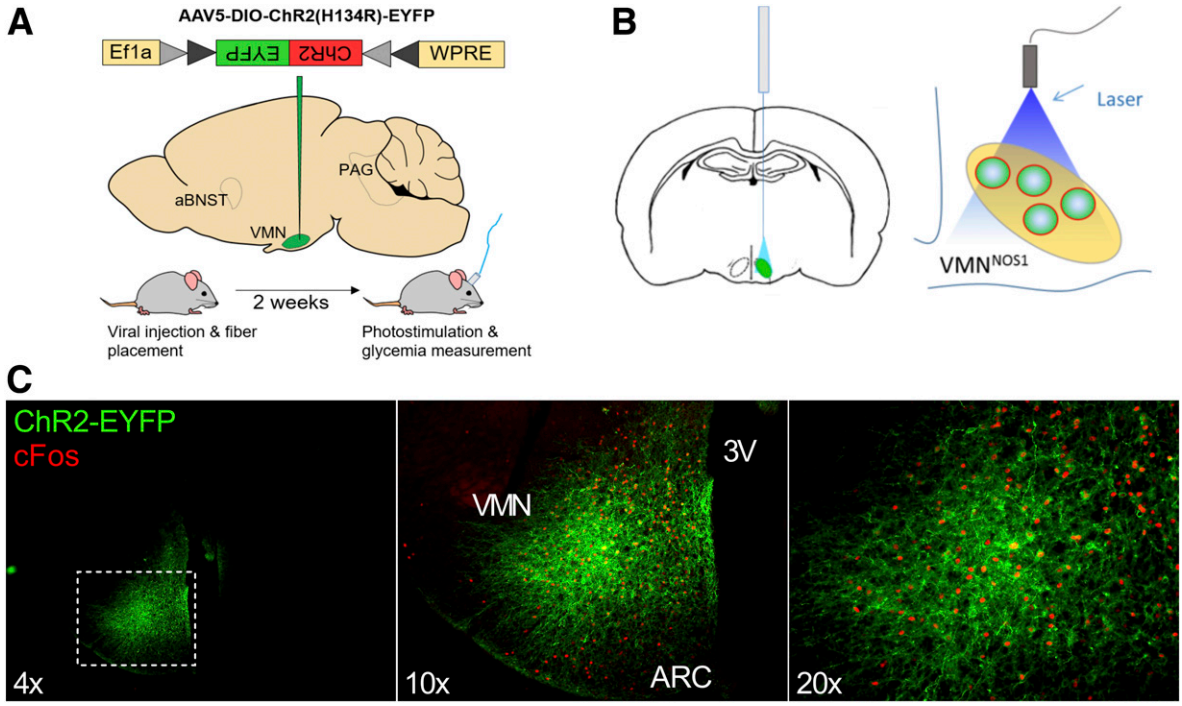

Figure 1—Strategy for photoactivation of VMN^{NOS1} neurons and verification of VMN targeting. Schematic demonstrating unilateral microinjection of the Cre-dependent ChR2-YFP or YFP control virus targeting the VMN of Nos1-Cre^{+} mice (*A*) and fiberoptic placement dorsal to the injection site (*B*). *C*: Representative images indicating unilateral infection and expression of ChR2-EYFP and light-induced c-Fos restricted to the VMN of Nos1-Cre^{+} mice. 3V, third ventricle; ARC, arcuate nucleus.

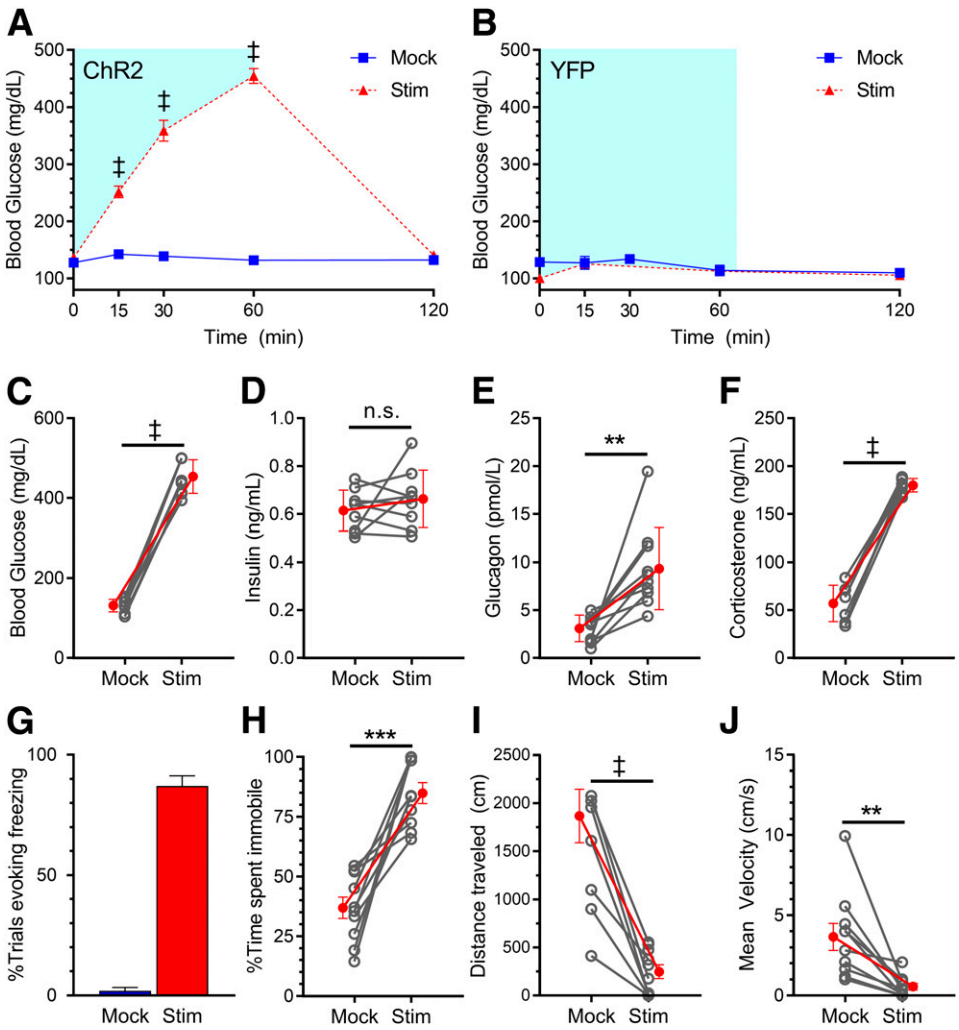

Figure 2—Photoactivation of VMN^{NOS1} neurons elicits both glucose CRRs and defensive freezing immobility. Blood glucose levels during unilateral laser off (mock) and laser-induced stimulation (Stim) of VMN^{NOS1} neurons in ChR2-YFP–injected ($n = 10$) (*A*) or YFP control–injected ($n = 3$) (*B*) animals. Blue shading represents the duration of laser stimulation. Blood glucose values from ChR2-YFP animals at the 60-min time point (*C*) during which tail blood was collected for measurement of insulin (*D*), glucagon (*E*), and corticosterone (*F*). *G*: Percentage of photoactivation trials evoking freezing. Percentage of time spent immobile (*H*), total distance traveled (*I*), and average velocity (*J*) during mock and photostimulation. Values are mean ± SEM. *P* values by two-way ANOVA (*A* and *B*) or two-tailed, paired Student *t* test (*C*–*J*). $^{**}P < 0.01$; $^{***}P < 0.001$; ‡$P < 0.0001$.

a corresponding decrease in the total distance traveled and average velocity (Fig. 2*I* and *J*). Importantly, these behaviors were not observed in Nos1-Cre^{+} animals that received a YFP control virus (Supplementary Video 2). Taken together, these data suggest that VMN^{NOS1} neuron activation elicits defensive freezing behaviors characteristic of generalized VMN stimulation and suggestive of the response to an underlying fearful emotional state.

VMN^{NOS1} Neurons Are Required for an Intact Glucagon Response to Insulin-Induced Hypoglycemia

To investigate the physiological role of VMN^{NOS1} neurons in the CRR, we asked whether activation of these neurons is required for the ability to recover from insulin-induced hypoglycemia. To this end, we used a complementary optogenetic approach in which a light-activated chloride-conducting channel was selectively expressed in VMN^{NOS1} neurons, such that light delivery hyperpolarizes and thereby reduces the firing of these neurons (11,29). Specifically, AAVDJ8-EF1-DIO-SwiChR$_{CA}$-TS-EYFP (hereafter called SwiChR-YFP) was microinjected bilaterally to the VMN of Nos1-Cre^{+} mice, followed by angled bilateral fiberoptic placement dorsal to each injection site (Fig. 3*A* and *B*).

We report that photoinhibition of VMN^{NOS1} neurons had no effect on blood glucose levels after saline injection (P = NS), suggesting that like VMN^{SF1} neurons, activation of VMN^{NOS1} neurons is not required for maintenance of normal blood glucose levels in the basal state. Unlike photoinhibition of VMN^{SF1} neurons (11), however, photoinhibition of VMN^{NOS1} neurons did not impair overall recovery from mild insulin-induced hypoglycemia (Fig. 3*C*), relative to mock controls. Nevertheless, the increase

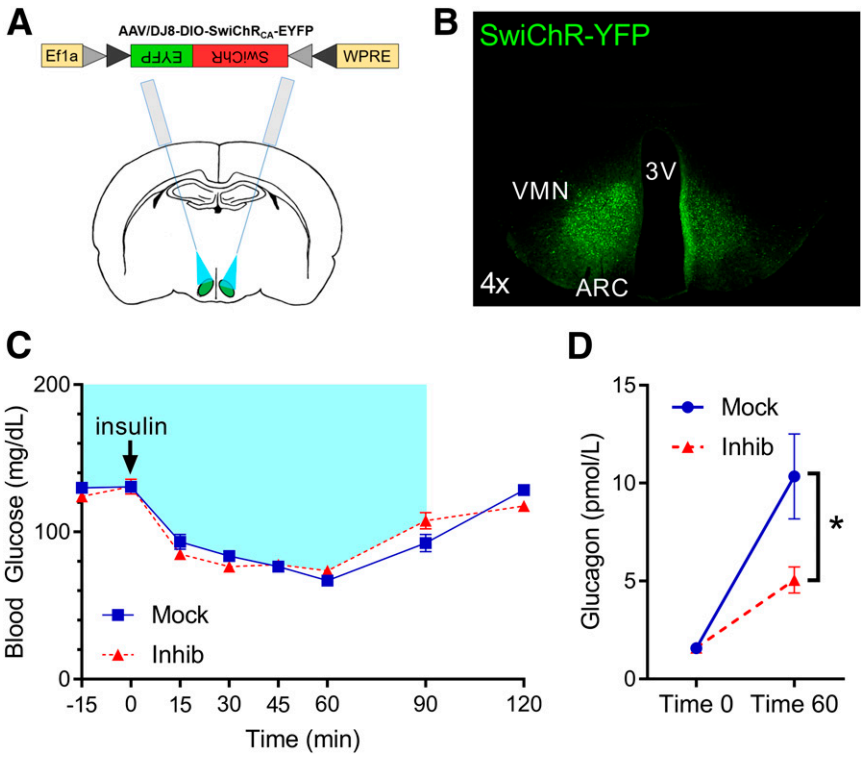

Figure 3—Photoinhibition of VMN^{NOS1} neurons selectively impairs glucagon responses during insulin-induced hypoglycemia. *A*: Schematic demonstrating bilateral microinjection of the Cre-dependent inhibitory SwiChR-YFP virus, and fiberoptic placement dorsal to the injection site, targeting the VMN of Nos1-Cre^{+} mice. *B*: Representative image of EYFP fluorescence showing bilateral infection and expression within the VMN of Nos1-Cre^{+} mice. *C*: Blood glucose levels in Nos1-Cre^{+} mice during bilateral laser off (Mock) or laser-induced inhibition (Inhib) of VMN^{NOS1} neurons. Blue shading represents duration of laser-induced inhibition. *D*: Changes in glucagon levels during insulin-induced hypoglycemia during mock and photoinhibition of VMN^{NOS1} neurons (n = 12 for all). Values are mean ± SEM. P values by two-way ANOVA. *$P < 0.05$. 3V, third ventricle; ARC, arcuate nucleus.

of circulating glucagon levels that normally occurs during hypoglycemia was blunted when VMN^{NOS1} neurons were silenced (Fig. 3*D*). In contrast, plasma corticosterone levels increased significantly from basal values in both groups and, unlike the blunted glucagon response, the magnitude of the effect was not affected by photoinhibition of VMN^{NOS1} neurons (t = 0 min, mock 82.3 ± 12.8 ng/mL vs. inhibition 85.8 ± 11.5 ng/mL, P = NS; t = 60 min, mock 118.1 ± 10.1 ng/mL vs. inhibition 122.2 ± 9.0 ng/mL, P = NS). A similar pattern of responses was observed when the study was repeated in separate cohorts of mice using a higher dose of insulin (1.5 units/kg) to induce a more severe degree of hypoglycemia. Thus, whereas photoinhibition of VMN^{NOS1} neurons again had no detectable effect on recovery from insulin-induced hypoglycemia relative to mock controls (blood glucose t = 60 min, mock 41.1 ± 6.9 ng/mL vs. inhibition 44.6 ± 7.3 mg/dL, P = NS), a blunted increase of plasma glucagon levels during hypoglycemia was observed once again (t = 60 min, mock 40.7 ± 5.1 ng/mL vs. inhibition 22.9 ± 3.9 pmol/L, $P < 0.05$). In contrast, photoinhibition of VMN^{NOS1} neurons did not alter the effect of hypoglycemia to raise plasma corticosterone levels (t = 60 min, mock 126.6 ± 6.6 ng/mL vs. inhibition 136.4 ± 6.3 ng/mL, P = NS). Taken together, these data demonstrate that activation of VMN^{NOS1} neurons is required for an intact glucagon response to insulin-induced hypoglycemia.

Identification of Downstream Projections of VMN^{NOS1} Neurons Mediating Glycemic and Behavioral Responses

As a first step to determine whether divergent glycemic and behavioral responses associated with VMN^{NOS1} activation can be dissociated from one another, we sought to identify projection fields of VMN^{NOS1} neurons tagged with fluorescently labeled channelrhodopsin virus. Consistent with previous data (11,30), fluorescently labeled projections were detected in both the ipsilateral aBNST (Fig. 4*A*, left) and both ipsilateral and contralateral PAG (Fig. 4*B*, left), areas implicated in autonomic control of metabolism and defensive behavior, respectively (22,23, 31,32). Moreover, neuron activation (as judged by c-Fos induction) was observed in both areas (Fig. 4*A* and *B*) after photoactivation of VMN^{NOS1} soma. Innervation of the PAG was particularly robust within its dorsolateral portion superior to the cerebral aqueduct.

Electrophysiological studies of the VMN have shown the presence of both glucose-excited (GE) and glucose-inhibited (GI) neurons in this area, which decrease and increase their firing in response to a fall in ambient glucose levels, respectively (33). Importantly, work from Fioramonti

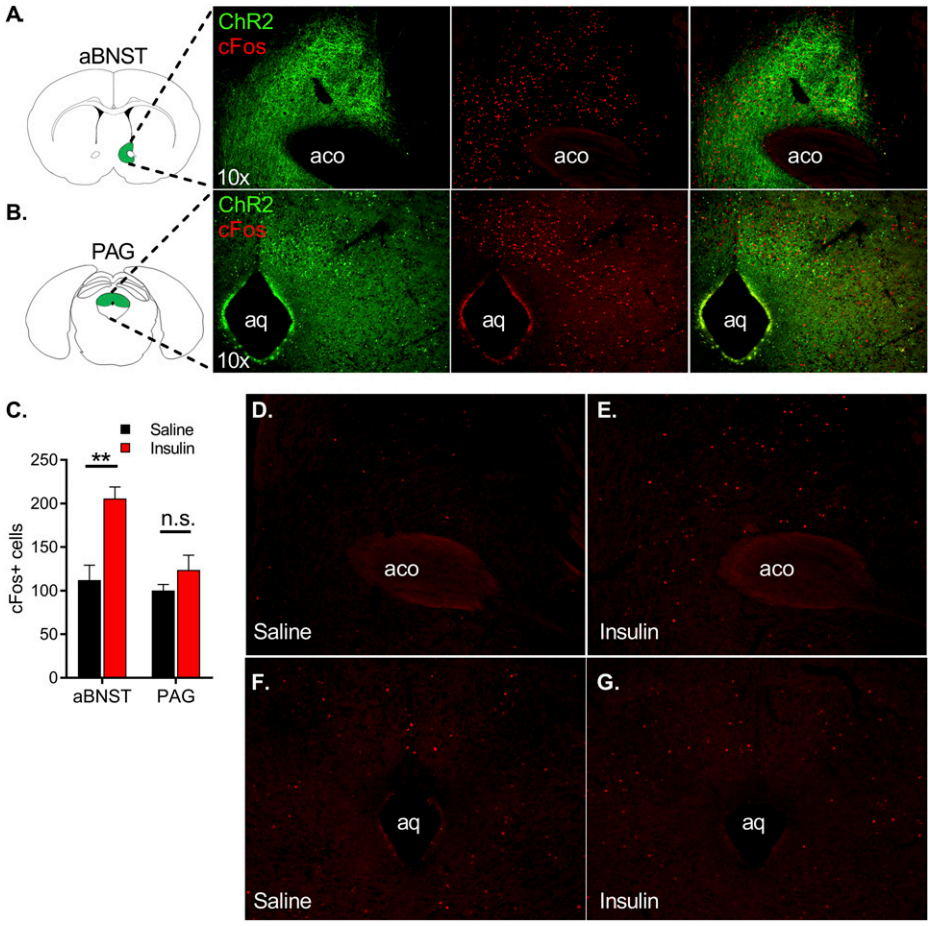

Figure 4—VMN^{NOS1} neurons project to and activate neurons in both the aBNST and the PAG, and insulin-induced hypoglycemia increases c-Fos expression within the aBNST. Fluorescently labeled projections of ChR2-expressing VMN^{NOS1} neurons in the aBNST (*A*, left panel) and PAG (*B*, left panel). Photoactivation of upstream VMN^{NOS1} neurons for 60 min elicits robust c-Fos expression in these regions (*A* and *B*, middle panel and merged right panel). *C*: Quantification of c-Fos^{+} cells in the aBNST and PAG of C57Bl/6J male mice after i.p. saline ($n = 4$) or insulin ($n = 6$; 1.5 units/kg). Representative magnification ×10 of c-Fos induction in the aBNST (*D* and *E*) and PAG (*F* and *G*) after i.p. saline (left) or insulin (right). Magnification 10×. Values are mean ± SEM. Two-tailed, unpaired Student *t* test for each brain region. $^{**}P < 0.01$. aco, anterior commissure; aq, cerebral aqueduct.

et al. (24) suggests that NOS1 neurons are predominantly GI, and activation of these neurons, alongside inhibition of GE neurons, in response to hypoglycemia may be required for the full CRR (24). Based on these data, and on evidence that VMN neurons are predominantly glutamatergic (12,34), we hypothesized that brain regions downstream of GI VMN^{NOS1} neurons would be activated during insulin-induced hypoglycemia.

To interrogate whether either the aBNST or PAG is activated during hypoglycemia, we exposed C57Bl/6J mice to insulin-induced hypoglycemia and evaluated c-Fos induction within these regions. Our data reproduce previous evidence that insulin-induced hypoglycemia activates neurons within the aBNST (31) but not within the PAG (Fig. 4*C*–*G*). We therefore hypothesized that selective activation of the VMN^{NOS1}→aBNST neurocircuit activates CRRs, whereas activation of the VMN^{NOS1}→PAG neurocircuit elicits the defensive freezing behaviors associated with VMN^{NOS1} activation.

To test this hypothesis, we used an optogenetics approach to stimulate the projection fields of VMN^{NOS1} neurons supplying the aBNST and the PAG. Specifically, AAV encoding Cre-dependent ChR2-YFP was microinjected unilaterally to the VMN of Nos1-Cre^{+} mice, followed by ipsilateral implantation of an optic fiber above projection fields within either the aBNST (Fig. 5*A*) or PAG (Fig. 6*A*) in separate cohorts of mice. In extension of our previous data (11), we found that photoactivation of VMN^{NOS1}→aBNST terminals recapitulated the effects of VMN^{NOS1} cell body activation to rapidly and reversibly raise blood glucose levels (Fig. 5*B*), a response accompanied by elevated plasma levels of both glucagon and corticosterone (Fig. 5*E* and *F*) and suppression of GSIS (Fig. 5*D*). Moreover, this effect occurred in the absence of the freezing immobility elicited by VMN^{NOS1} cell body stimulation (Fig. 5*G*–*J* and Supplementary Video 3). Collectively, these findings corroborate our previous data implicating the subset of aBNST-projecting VMN

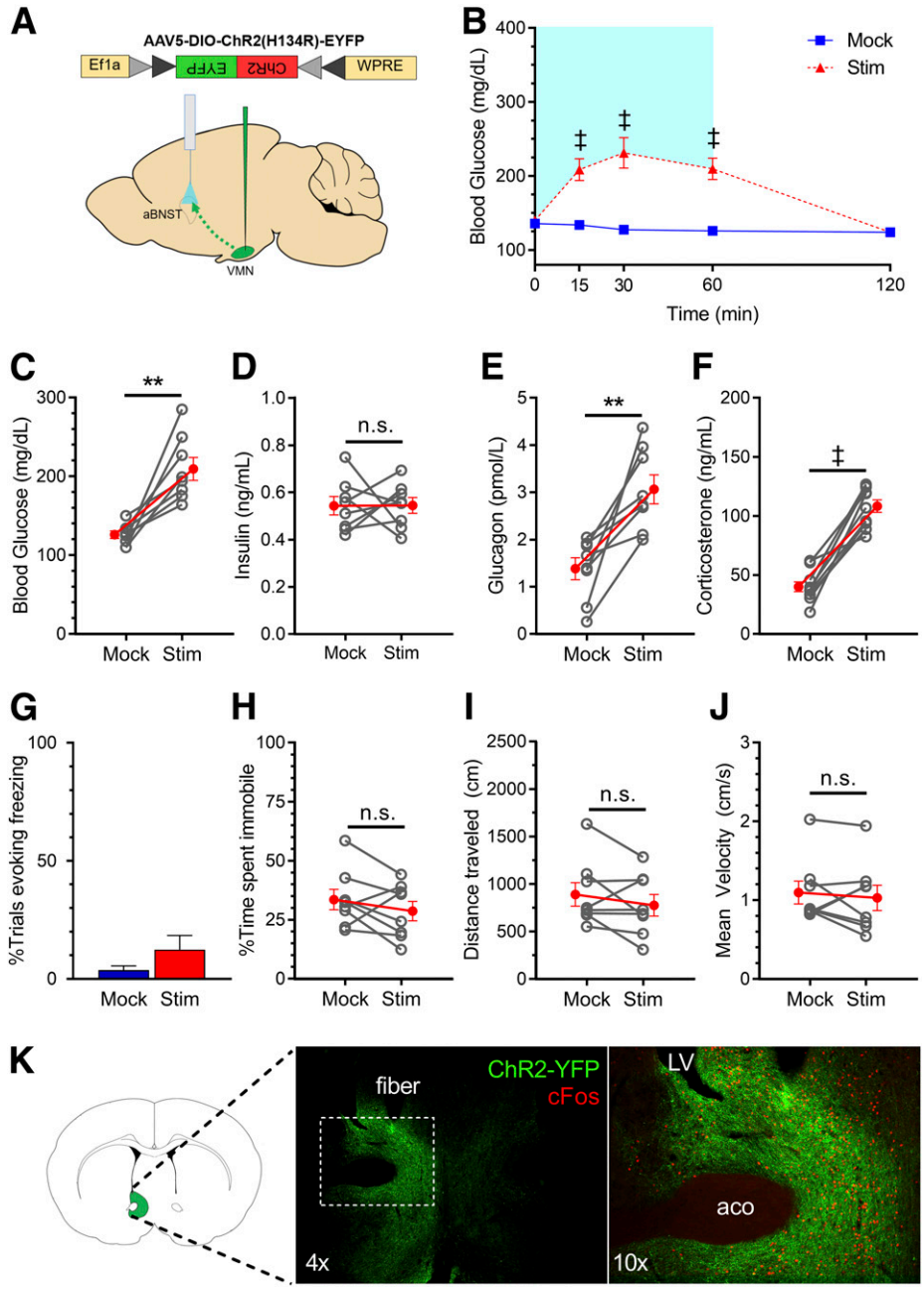

Figure 5—Photoactivation of VMN^{NOS1}→aBNST projections selectively promotes hyperglycemia by activating CRRs, without eliciting freezing immobility. *A*: Schematic for laser off (mock) or laser-induced stimulation (Stim) of VMN^{NOS1} terminals in the aBNST (VMN^{NOS1}→aBNST). *B*: Blood glucose levels during ipsilateral mock and photoactivation of VMN^{NOS1}→aBNST terminals. Blue shading represents the duration of laser-induced stimulation. Blood glucose values at the 60-min time point (*C*) during which tail blood was collected for measurement of insulin (*D*), glucagon (*E*), and corticosterone (*F*). *G*: Percentage of photoactivation trials evoking freezing. Percentage of time spent immobile (*H*), total distance traveled (*I*), and average velocity (*J*) during mock and photostimulation ($n = 8$ for all). *K*: Representative image indicating terminals of ChR2-expressing VMN^{NOS1} neurons within the ipsilateral aBNST and light-induced c-Fos within the aBNST. Values are mean ± SEM. *P* values by two-way ANOVA (*B*) and two-tailed, paired Student *t* test (*C*–*J*). $^{**}P < 0.01$; ‡$P < 0.0001$. aco, anterior commissure; LV, lateral ventricle.

neurons as components of a neurocircuit involved in glucose counterregulation.

We also report that, as predicted, photoactivation of VMN^{NOS1}→PAG projections reliably and robustly reproduced the freezing immobility seen upon VMN^{NOS1} activation (Fig. 6*G*–*J* and Supplementary Video 4). Although we also found that photoactivation of VMN^{NOS1}→PAG projections elicited hyperglycemia (Fig. 6*B*), activation of these projections failed to increase glucagon secretion (Fig. 6*E*). Although activation of this circuit is clearly capable of inducing both hyperglycemia and behavioral fear responses, it does not fully engage the prototypic

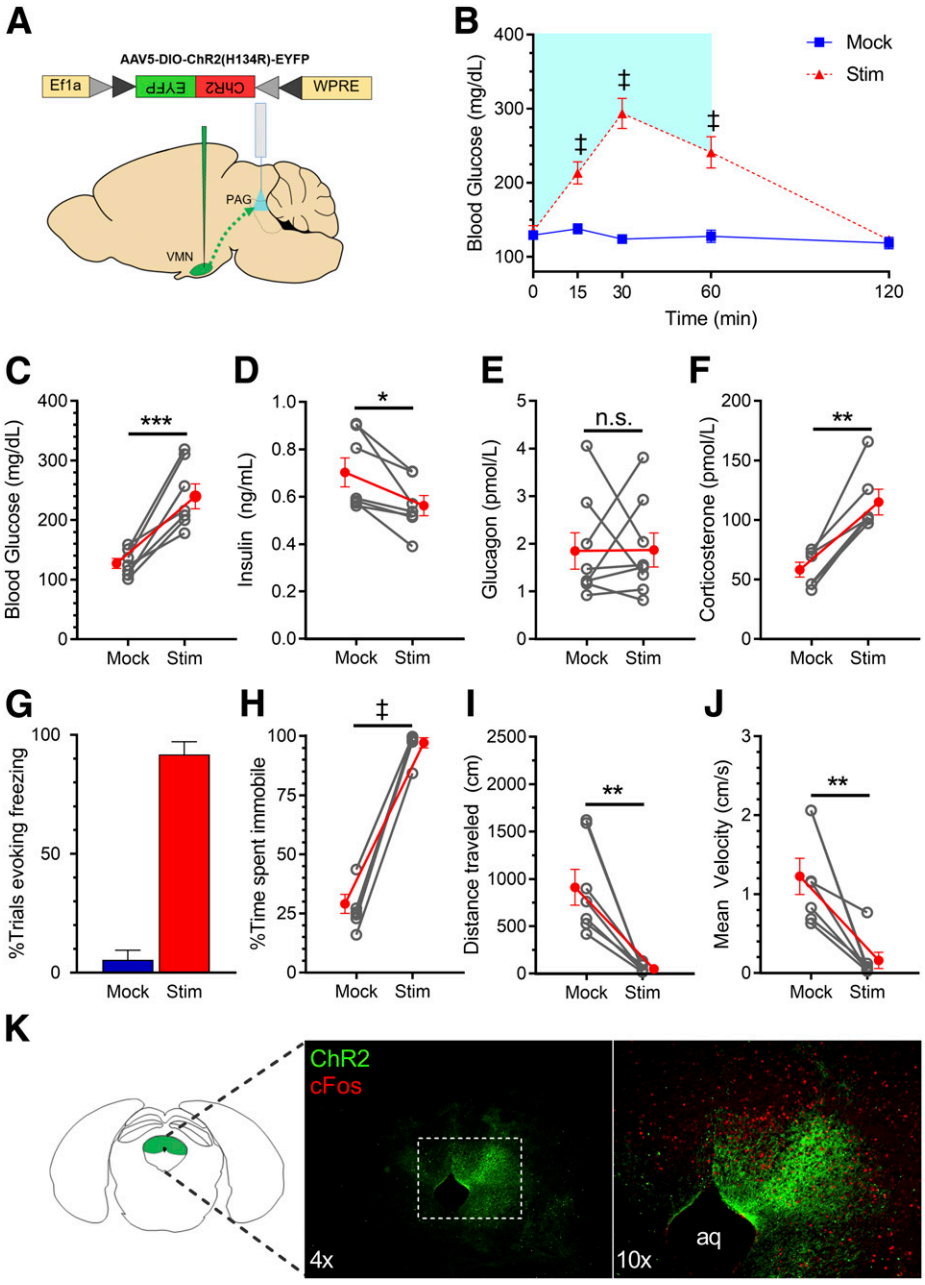

Figure 6—Photoactivation of VMN^{NOS1}→PAG projections elicits defensive freezing immobility. *A*: Schematic for laser off (mock) or light-induced stimulation (Stim) of VMN^{NOS1} terminals in the PAG (VMN^{NOS1}→PAG). *B*: Blood glucose levels during ipsilateral mock and photoactivation of VMN^{NOS1}→PAG terminals. Blue shading represents the duration of laser-induced stimulation. Blood glucose values at the 60-min time point (*C*) during which tail blood was collected for measurement of insulin (*D*), glucagon (*E*), and corticosterone (*F*). *G*: Percentage of photoactivation trials evoking freezing. Percentage of time spent immobile (*H*), total distance traveled (*I*), and average velocity (*J*) during mock and photostimulation ($n = 8$ for all). *K*: Representative image indicating terminals of ChR2-expressing VMN^{NOS1} neurons in the PAG and light-induced c-Fos within the PAG. Values are mean ± SEM. *P* values by two-way ANOVA (*B*) and two-tailed, paired Student *t* test (*C*–*J*). *$P < 0.05$; **$P < 0.01$; ***$P < 0.001$; ‡$P < 0.0001$. aq, cerebral aqueduct.

CRR, as seen after activation of the VMN^{NOS1}→aBNST projection.

DISCUSSION

The brain requires a continuous supply of glucose to support its energy demands and, in response to an acute energy deficit (e.g., hypoglycemia), it engages rapid, potent, and highly integrated neuroendocrine and autonomic responses that return blood glucose into the normal range. Although many brain areas participate in this response (35), we recently reported that activation of the subset of VMN neurons that express SF1 is both necessary and sufficient for intact CRRs in response to insulin-induced hypoglycemia (11). Here, we extend this work

by showing that the subset of these VMN neurons that express NOS1 contributes to this effect. Our findings show that although inhibition of VMN^{NOS1} neurons blunts the glucagon response to insulin-induced hypoglycemia, neither activation of the hypothalamic-pituitary-adrenal (HPA) axis nor recovery of blood glucose to normal levels were affected, providing further evidence that multiple, redundant central and peripheral pathways contribute to the defense against hypoglycemia (36). Conversely, we found that selective photoactivation of VMN^{NOS1} neurons in otherwise normal mice causes robust hyperglycemia characterized by activation of CRRs normally reserved for the response to hypoglycemia (inhibition of GSIS and increased secretion of both glucagon and corticosterone; epinephrine also plays a key role in glucose counterregulation, however, we were unable to measure epinephrine in the current studies). However, since photoactivation of VMN^{NOS1} neurons also induces defensive behaviors (i.e., freezing immobility), the question is raised as to whether the behavioral and metabolic responses are inextricably linked to one another or instead involve neuronal projections to distinct brain areas. Our findings support the latter hypothesis. Specifically, we found that activation of VMN^{NOS1} projections to the aBNST (VMN^{NOS1}→aBNST) induces CRRs and hyperglycemia, whereas defensive behavioral responses were only observed after activation of VMN^{NOS1} terminals in the PAG (VMN^{NOS1}→PAG). Together, these findings suggest that the subset of VMN^{NOS1} neurons that project to the aBNST is involved in glucose counterregulation, whereas the VMN^{NOS1}→PAG pathway is linked to fear-induced behavioral responses.

Although compelling evidence implicates the VMN in both autonomic and neuroendocrine CRRs that drive recovery from hypoglycemia (8–10,37,38), activation of the VMN also elicits "fight or flight" (39,40), defensive (16,17), and aggressive (41–43) behaviors, and the extent to which the glycemic response is secondary to or is an inherent component of the behavioral stress response is unknown. Here, we considered the possibility that these divergent biological functions reflect the activity of distinct subsets of VMN neurons that project to discrete downstream brain regions. Our focus on VMN neurons expressing NOS1 is based on evidence that decreased glucose activates NOS1 and increases NO production in mediobasal hypothalamus (7) and that NOS1 is required for intact glucose sensing by GI neurons in the VMN (24). Moreover, mediobasal hypothalamus injection of a nonselective NOS inhibitor impaired the CRR and blunted the recovery from insulin-induced hypoglycemia (24), and the CRR to hypoglycemia is impaired in NOS1-deficient mice (24). Last, VMN^{NOS1} neurons are a subset of VMN^{SF1} neurons, activation of which robustly engages CRRs. We therefore interpret our findings to suggest that *1*) photoinhibition of VMN^{NOS1} neurons impairs glucagon, but not corticosterone, responses during insulin-induced hypoglycemia, and *2*) photoactivation of VMN^{NOS1} neurons induces diabetes-range hyperglycemia in otherwise normal mice via a mechanism involving activation of CRRs to suggest an important role for VMN^{NOS1} neurons to drive specific components of the CRR to hypoglycemia. Although the mechanism(s) that mediates each of these responses remains to be elucidated, long-standing evidence suggests that the islet is under autonomic control (44), and increased sympathetic activity both increases glucagon (45) and inhibits insulin secretion (46).

Several lines of evidence also link activation of VMN neurons to "fight or flight" and other behavioral responses to fearful or threatening stimuli. For example, neurons within the VMNvl are activated during escape and defensive responses to an aggressive conspecific, and predator exposure activates neurons in the VMNdm; conversely, painful stimuli (e.g., foot shock) do not activate VMN neurons (39). The hypothesis that specific VMN neuronal populations are recruited during predator and social fear and that similar fear behaviors recruit different brain circuits is also supported by data from pharmacogenetics studies showing that inhibition of the VMNvl decreases defensive responses to an aggressive conspecific (39), whereas activation of a specific subset of VMNvl neurons (marked by expression of estrogen receptor 1) induces mating behavior and fighting in rodents (41,43). By comparison, pharmacogenetic inhibition of the VMNdm impairs defensive responses to predators (39), whereas photoactivation of VMNdm neurons induces flight and freezing behavior (16,17). These behaviors also appear to occur in a scalable manner, with less intense stimulation inducing freezing and more intense stimulation evoking activity bursts (16). Taken together, these studies suggest that the VMNdm, a region also implicated in the control of energy homeostasis and metabolism (20,47), is involved in predator fear and other defensive behaviors, whereas the VMNvl is a region involved in sexual and aggressive behavior and social fear (40–43).

As a first step to investigate whether the subset of VMN^{NOS1} neurons involved in glucose counterregulation are causally linked to these behavioral responses, we characterized the downstream projection fields of these neurons using a fluorescently labeled channelrhodopsin. Consistent with work from us and others, the aBNST and PAG receive the heaviest projections from VMN^{NOS1} neurons (11,30,48). Our finding that photostimulation of the subset of VMN^{NOS1} neurons that project to the aBNST mimics the glycemic response elicited by VMN^{NOS1} neuronal stimulation (including increases of plasma glucagon and corticosterone levels and inhibition of GSIS), but does not induce defensive or other detectable behaviors, provides compelling evidence that the VMN^{NOS1}→aBNST projection constitutes a neurocircuit involved in glycemic control but not in behavioral regulation. Implicit in this conclusion is not only that a behavioral response is not required for VMN neuron activation to elicit robust hyperglycemia but also that a distinct VMN^{NOS1} neuronal projection must drive the behavioral response.

Among various VMN projection fields with the potential to mediate defensive behaviors, the PAG stands out because *1*) this brain area is activated in response to a wide variety of threats (49,50); *2*) impaired PAG function diminishes the expression of defensive behaviors, including freezing, risk assessment, and flight (39,51); *3*) stimulation of the PAG is sufficient to induce defensive responses, including freezing, escape, and flight (52); and *4*) this brain area (particularly, its dorsal columns) receives input from the VMN (11,30,48). Our finding that photostimulation of the subset of VMN^{NOS1} neurons that project to the PAG elicits defensive behaviors is consistent with previous evidence linking projections from the VMNdm to the dorsal region of the PAG in this behavior, whereas projections to the anterior hypothalamic area are implicated in risk assessment and flight (17).

Given this evidence linking the VMN→PAG projection in defensive behavior, it came as something of a surprise that hyperglycemia is also induced by photostimulation of VMN^{NOS1} neurons that project to the PAG, especially since activation of VMN^{SF1}→PAG projections does not have this effect (11). The mechanism driving this response is not identical with that engaged by projections of VMN^{NOS1} neurons to the aBNST; however, because it raised corticosterone levels (reflecting activation of the HPA axis), glucagon secretion was not increased. Furthermore, we report that insulin-induced hypoglycemia activates neurons in the aBNST but not the PAG. We interpret these collective findings to suggest that activation of the VMN^{NOS1}→PAG projection induces a nonspecific stress response marked by defensive behaviors, activation of the HPA axis, and hyperglycemia but does not participate in glucose counterregulation per se. This hypothesis warrants additional investigation, particularly given recent evidence suggesting a role for the PAG in mobilizing glucose during exposure to noxious or painful stimuli (32).

In conclusion, we report that activation of the subset of VMN neurons that express NOS1 rapidly induces diabetes-range hyperglycemia owing to the combination of a marked increase in glucagon and corticosterone secretion and inhibition of GSIS, characteristic of the CRR to hypoglycemia. We further show that activation of the specific subset of VMN^{NOS1} neurons that project to the aBNST is sufficient to engage the same glucoregulatory response, while having no detectable behavioral phenotype, whereas VMN^{NOS1} neurons that project to the PAG are implicated in defensive behaviors. Further insight into these VMN neurocircuits will inform our understanding of both hypoglycemia and its complications in patients with diabetes (53) and mechanisms underlying the "fight or flight" response and other defensive behaviors.

Acknowledgments. The authors acknowledge the technical expertise provided by Trista Harvey (University of Washington) for animal and IHC studies, Kayoko Ogimoto and Jarrell Nelson (NORC Energy Balance Core) for supporting optogenetics studies, and the technical assistance provided by Madison Baird from the laboratory of Larry Zweifel (University of Washington) for behavioral analysis with Ethovision (Noldus).

Funding. This work was supported by the National Institute of Diabetes and Digestive and Kidney Diseases (NIDDK) grants F31-DK-113673 (C.L.F.), T32-GM-095421 (C.L.F.), DK-083042, DK-101997 (M.W.S.), and DK-089056 (G.J.M.) and the NIDDK-funded Nutrition Obesity Research Center (DK-035816) and Diabetes Research Center (DK-017047) at the University of Washington.

Duality of Interest. No potential conflicts of interest relevant to this article were reported.

Author Contributions. C.L.F. designed research studies, conducted experiments, acquired and analyzed data, and wrote and edited the manuscript. M.E.M., K.R.V., D.A., and A.T. conducted experiments, acquired and analyzed data, and edited the manuscript. V.D. and B.A.P. conducted experiments and acquired data. M.W.S. and G.J.M. designed research studies, analyzed data, and wrote and edited the manuscript. G.J.M. is the guarantor of this work and, as such, had full access to all the data in the study and takes responsibility for the integrity of the data and the accuracy of the data analysis.

Prior Presentation. Aspects of this work were presented at the 77th Scientific Sessions of the American Diabetes Association, San Diego, CA, 9–13 June 2017, and the Keystone Symposium (January 2018).

References

1. Ritter RC, Slusser PG, Stone S. Glucoreceptors controlling feeding and blood glucose: location in the hindbrain. Science 1981;213:451–452
2. Saberi M, Bohland M, Donovan CM. The locus for hypoglycemic detection shifts with the rate of fall in glycemia: the role of portal-superior mesenteric vein glucose sensing. Diabetes 2008;57:1380–1386
3. Routh VH, Donovan CM, Ritter S. 2. Hypoglycemia detection. Transl Endocrinol Metab 2012;3:47–87
4. Beall C, Ashford ML, McCrimmon RJ. The physiology and pathophysiology of the neural control of the counterregulatory response. Am J Physiol Regul Integr Comp Physiol 2012;302:R215–R223
5. Cryer PE. Mechanisms of hypoglycemia-associated autonomic failure in diabetes. N Engl J Med 2013;369:362–372
6. Heller SR, Cryer PE. Reduced neuroendocrine and symptomatic responses to subsequent hypoglycemia after 1 episode of hypoglycemia in nondiabetic humans. Diabetes 1991;40:223–226
7. Canabal DD, Song Z, Potian JG, Beuve A, McArdle JJ, Routh VH. Glucose, insulin, and leptin signaling pathways modulate nitric oxide synthesis in glucose-inhibited neurons in the ventromedial hypothalamus. Am J Physiol Regul Integr Comp Physiol 2007;292:R1418–R1428
8. Frohman LA, Bernardis LL. Effect of hypothalamic stimulation on plasma glucose, insulin, and glucagon levels. Am J Physiol 1971;221:1596–1603
9. Dubuc PU, Leshin LS, Willis PL. Glucose and endocrine responses to hypothalamic electrical stimulation in rats. Am J Physiol 1982;242:R220–R226
10. Borg MA, Sherwin RS, Borg WP, Tamborlane WV, Shulman GI. Local ventromedial hypothalamus glucose perfusion blocks counterregulation during systemic hypoglycemia in awake rats. J Clin Invest 1997;99:361–365
11. Meek TH, Nelson JT, Matsen ME, et al. Functional identification of a neurocircuit regulating blood glucose. Proc Natl Acad Sci U S A 2016;113:E2073–E2082
12. Tong Q, Ye C, McCrimmon RJ, et al. Synaptic glutamate release by ventromedial hypothalamic neurons is part of the neurocircuitry that prevents hypoglycemia. Cell Metab 2007;5:383–393
13. Garfield AS, Shah BP, Madara JC, et al. A parabrachial-hypothalamic cholecystokinin neurocircuit controls counterregulatory responses to hypoglycemia. Cell Metab 2014;20:1030–1037
14. Hashikawa Y, Hashikawa K, Falkner AL, Lin D. Ventromedial hypothalamus and the generation of aggression. Front Syst Neurosci 2017;11:94
15. Anderson DJ. Optogenetics, sex, and violence in the brain: implications for psychiatry. Biol Psychiatry 2012;71:1081–1089

16. Kunwar PS, Zelikowsky M, Remedios R, et al. Ventromedial hypothalamic neurons control a defensive emotion state. eLife 2015;4:1–30
17. Wang L, Chen IZ, Lin D. Collateral pathways from the ventromedial hypothalamus mediate defensive behaviors. Neuron 2015;85:1344–1358
18. Falkner AL, Grosenick L, Davidson TJ, Deisseroth K, Lin D. Hypothalamic control of male aggression-seeking behavior. Nat Neurosci 2016;19:596–604
19. Chan O, Sherwin R. Influence of VMH fuel sensing on hypoglycemic responses. Trends Endocrinol Metab 2013;24:616–624
20. Choi YH, Fujikawa T, Lee J, Reuter A, Kim KW. Revisiting the ventral medial nucleus of the hypothalamus: the roles of SF-1 neurons in energy homeostasis. Front Neurosci 2013;7:71
21. Choi DC, Furay AR, Evanson NK, Ostrander MM, Ulrich-Lai YM, Herman JP. Bed nucleus of the stria terminalis subregions differentially regulate hypothalamic-pituitary-adrenal axis activity: implications for the integration of limbic inputs. J Neurosci 2007;27:2025–2034
22. Crestani CC, Alves FH, Gomes FV, Resstel LB, Correa FM, Herman JP. Mechanisms in the bed nucleus of the stria terminalis involved in control of autonomic and neuroendocrine functions: a review. Curr Neuropharmacol 2013;11:141–159
23. Benarroch EE. Periaqueductal gray: an interface for behavioral control. Neurology 2012;78:210–217
24. Fioramonti X, Marsollier N, Song Z, et al. Ventromedial hypothalamic nitric oxide production is necessary for hypoglycemia detection and counterregulation. Diabetes 2010;59:519–528
25. Murphy BA, Fakira KA, Song Z, Beuve A, Routh VH. AMP-activated protein kinase and nitric oxide regulate the glucose sensitivity of ventromedial hypothalamic glucose-inhibited neurons. Am J Physiol Cell Physiol 2009;297:C750–C758
26. Grishagin IV. Automatic cell counting with ImageJ. Anal Biochem 2015;473:63–65
27. Sanford CA, Soden ME, Baird MA, et al. A central amygdala CRF circuit facilitates learning about weak threats. Neuron 2017;93:164–178
28. Ulrich-Lai YM, Herman JP. Neural regulation of endocrine and autonomic stress responses. Nat Rev Neurosci 2009;10:397–409
29. Berndt A, Yeun Lee S, Ramakrishnan C, Deisseroth K. Structure-guided transformation of channelrhodopsin into a light-activated chloride channel. Science 2014;344:420–424
30. Canteras NS, Simerly RB, Swanson LW. Organization of projections from the ventromedial nucleus of the hypothalamus: a Phaseolus vulgaris-leucoagglutinin study in the rat. J Comp Neurol 1994;348:41–79
31. Niimi M, Sato M, Tamaki M, Wada Y, Takahara J, Kawanishi K. Induction of Fos protein in the rat hypothalamus elicited by insulin-induced hypoglycemia. Neurosci Res 1995;23:361–364
32. Flak JN, Arble D, Pan W, et al. A leptin-regulated circuit controls glucose mobilization during noxious stimuli. J Clin Invest 2017;127:3103–3113
33. Routh VH. Glucose sensing neurons in the ventromedial hypothalamus. Sensors (Basel) 2010;10:9002–9025
34. Chachlaki K, Malone SA, Qualls-Creekmore E, et al. Phenotyping of nNOS neurons in the postnatal and adult female mouse hypothalamus. J Comp Neurol 2017;525:3177–3189
35. Ritter S, Li A-J, Wang Q, Dinh TT. Minireview: the value of looking backward: the essential role of the hindbrain in counterregulatory responses to glucose deficit. Endocrinology 2011;152:4019–4032
36. McCrimmon R. The mechanisms that underlie glucose sensing during hypoglycaemia in diabetes. Diabet Med 2008;25:513–522
37. Borg WP, During MJ, Sherwin RS, Borg MA, Brines ML, Shulman GI. Ventromedial hypothalamic lesions in rats suppress counterregulatory responses to hypoglycemia. J Clin Invest 1994;93:1677–1682
38. Borg WP, Sherwin RS, During MJ, Borg MA, Shulman GI. Local ventromedial hypothalamus glucopenia triggers counterregulatory hormone release. Diabetes 1995;44:180–184
39. Silva BA, Mattucci C, Krzywkowski P, et al. Independent hypothalamic circuits for social and predator fear. Nat Neurosci 2013;16:1731–1733
40. Spiteri T, Musatov S, Ogawa S, Ribeiro A, Pfaff DW, Ågmo A. The role of the estrogen receptor α in the medial amygdala and ventromedial nucleus of the hypothalamus in social recognition, anxiety and aggression. Behav Brain Res 2010;210:211–220
41. Lee H, Kim D-W, Remedios R, et al. Scalable control of mounting and attack by Esr1+ neurons in the ventromedial hypothalamus. Nature 2014;509:627–632
42. Lin D, Boyle MP, Dollar P, et al. Functional identification of an aggression locus in the mouse hypothalamus. Nature 2011;470:221–226
43. Falkner AL, Dollar P, Perona P, Anderson DJ, Lin D. Decoding ventromedial hypothalamic neural activity during male mouse aggression. J Neurosci 2014;34:5971–5984
44. Begg DP, Woods SC. Interactions between the central nervous system and pancreatic islet secretions: a historical perspective. Adv Physiol Educ 2013;37:53–60
45. Taborsky GJ Jr., Mundinger TO. Minireview: the role of the autonomic nervous system in mediating the glucagon response to hypoglycemia. Endocrinology 2012;153:1055–1062
46. Thorens B. Neural regulation of pancreatic islet cell mass and function. Diabetes Obes Metab 2014;16(Suppl. 1):87–95
47. Dhillon H, Zigman JM, Ye C, et al. Leptin directly activates SF1 neurons in the VMH, and this action by leptin is required for normal body-weight homeostasis. Neuron 2006;49:191–203
48. Gross CT, Canteras NS. The many paths to fear. Nat Rev Neurosci 2012;13:651–658
49. Motta SC, Goto M, Gouveia FV, Baldo MVC, Canteras NS, Swanson LW. Dissecting the brain's fear system reveals the hypothalamus is critical for responding in subordinate conspecific intruders. Proc Natl Acad Sci U S A 2009;106:4870–4875
50. Vianna DML, Brandão ML. Anatomical connections of the periaqueductal gray: specific neural substrates for different kinds of fear. Braz J Med Biol Res 2003;36:557–566
51. Hunsperger RW. Affective behavior patterns elicited by electrical stimulation of the brain stem and forebrain. J Physiol (Paris) 1963;55:45–97 [in French]
52. Quintino-dos-Santos JW, Müller CJT, Bernabé CS, Rosa CA, Tufik S, Schenberg LC. Evidence that the periaqueductal gray matter mediates the facilitation of panic-like reactions in neonatally-isolated adult rats. PLoS One 2014;9:e90726
53. Frier BM. Hypoglycaemia in diabetes mellitus: epidemiology and clinical implications. Nat Rev Endocrinol 2014;10:711–722.